Chemical reaction and Schottky-barrier formation at the Ir/Si interface

M. Wittmer, P. Oelhafen,* and K. N. Tu
IBM Thomas J. Watson Research Center, P.O. Box 218, Yorktown Heights, New York 10598
(Received 10 December 1986)

The initial stages of formation of the Ir/Si interface were investigated with ultraviolet and x-ray photoelectron spectroscopy. It was found that submonolayer coverages of iridium change the (2×1) reconstruction of the clean silicon surface and increase the band bending. With increasing coverage a bilayer structure forms consisting of an interfacial layer of IrSi-like silicide and an overlayer of pure iridium. The Schottky barrier is fully developed after deposition of the first monolayer of iridium. By annealing a thin film of iridium deposited on silicon in UHV in the temperature range of 400–1100 °C we demonstrate the consecutive formation of three silicide compounds in the sequence IrSi, $IrSi_x$ ($x\simeq1.6$), and $IrSi_3$ and the concomitant transitions from metallic to semiconducting and semiconducting to metallic behavior. Finally, we show that the barrier heights of the iridium silicides on silicon do not obey the simple Schottky model and compare our photoelectron results with current theoretical models of the Schottky barrier.

I. INTRODUCTION

The electronic properties of transition-metal–silicon interfaces are subjects of continuing interest for both fundamental and practical reasons. Such interfaces find a widespread application as Ohmic contacts and Schottky-barrier diodes in microelectronic devices. Though the fabrication of reproducible and reliable metal-silicon interfaces is easily achieved today, an unified picture of the nature of the Schottky barrier and the chemical trends in the variations of the barrier height are still lacking. This situation has stimulated intensive experimental[1–13] and theoretical[14–18] investigations of the chemical bonding and the electronic structure of transition-metal–silicon interfaces. In spite of the large number of such studies, the physical and chemical mechanisms underlying the barrier height of a metal-silicon interface are not yet fully understood.

We have chosen to study the Ir/Si(100) interface because its electronic structure is of particular interest for the following reasons: A study of the growth kinetics of iridium silicide thin films has shown that three stoichiometric iridium silicide compounds, IrSi, $IrSi_x$ ($x\simeq1.6$), and $IrSi_3$ form sequentially, i.e., only one of them grows at any time in a specific temperature range.[19] In addition, iridium silicide Schottky diodes on *n*-type silicon exhibit the highest barrier height (0.93 eV) known to date of any silicides.[20] Thus, the electronic properties of iridium-silicide–silicon interfaces and their dependence on compositional changes are of great interest in a quantitative understanding of the Schottky barrier. Such a study has not yet been carried out.

Recently, we have reported on the electronic structure of the three bulk iridium silicide compounds.[21] We concluded from the observed narrowing of the iridium *d* band and the concomitant broadening of the Si $2p$ core levels in the silicides that the bonding in these compounds is caused by a hybridization of the Ir *d* states and the Si *sp* hybrids. This type of bonding has also been reported for $3d$ and $4d$ transition-metal silicides.[3,6,7] In contrast, we did not observe a *d*-band shift as reported in other transition-metal silicides. But we found that IrSi and $IrSi_3$ are metallic and $IrSi_x$ ($x\simeq1.6$) is semiconducting.[22] We proposed a model to explain this difference in terms of chemical trends in the bonding of iridium silicide compounds. In the following we will refer to this work as paper I.

In this paper we present an ultraviolet photoelectron (UPS) and x-ray photoelectron spectroscopy (XPS) study of the initial stages of iridium-silicon interface formation. We will show that the properties of the Ir/Si(100) interface are dominated by compound formation, pointing out the strong reactive character of this interface. By annealing of a thin iridium film deposited on a silicon substrate at successively higher temperatures, we will demonstrate the consecutive formation of the three silicide compounds in the order of IrSi, $IrSi_x$ ($x\simeq1.6$), and $IrSi_3$, and reveal the concomitant transitions from metallic to semiconducting and semiconducting to metallic behavior. Such a behavior has not been previously reported for a series of transition-metal silicides. Finally, we will correlate the measured work function of the three silicides with their barrier height values published in the literature[20] and compare the results with existing models of the Schottky barrier.

II. EXPERIMENTAL

The silicon substrates used throughout the course of this work were cut from *n*-type wafers of (100) orientation and 5 Ω cm resistivity. Cleaning of the substrates was performed in an ultrahigh vacuum (UHV) preparation chamber by a repeated sputtering with 1000-eV Ar^+ ions and annealing at about 850 °C for 3 min. The pressure rise during annealing was kept below 2×10^{-9} Torr. A sharp (2×1) two-domain low-energy electron diffraction (LEED) pattern was obtained with this cleaning procedure. The silicon substrates were then ready for

transfer into the analysis chamber.

The iridium overlayers were deposited by direct sublimation from a resistively heated iridium filament. Care was needed due to the relatively small difference in temperature between the onset of sublimation and the melting point of iridium (2410 °C). Best results were obtained by using 7 turns out of 0.25-mm-diam. iridium wire of 99.9% purity wound with a diameter of 2.5 mm. Stable deposition rates were achieved by passing a constant current of 5.6—6.0 A through the filament. The filament was supported in a cylindrical housing together with a quartz-crystal thickness monitor. Deposition of iridium onto the sample was performed through a shutter operated window. The thickness of the deposited film was monitored by the frequency deviation of a quartz-crystal oscillator. Water cooling of the quartz-crystal monitor prevented frequency shifts due to heating of the crystal. Calibration of the thickness in terms of frequency deviation was carried out by analyzing deposited layers with Rutherford backscattering (RBS) spectrometry.[23] The accuracy of the thickness calibration was 0.1 Å and a typical deposition rate was 1 Å/min. In the following we will be referring to film thicknesses in the order of 0.1 Å. Such thicknesses are obtained from the frequency deviation of the quartz-crystal oscillator and correspond to about 0.1 ML of pseudomorphic growth of Ir on Si(100). One filament lasted for iridium depositions of about 80 Å before it failed.

Annealing of the deposited iridium films was performed inside the analysis chamber by resistively heating the Si substrate. The annealing temperature was monitored with an Ircon Model No. 300 infrared pyrometer. The calibration of the pyrometer for different emittances of the deposited layers has been described in paper I. The accuracy of the temperature measurement was estimated to be ±25 °C.

Photoemission measurements were performed in an angle-resolved spectrometer Model No. ADES 400 by Vacuum Generators, Inc. The resulting energy resolutions were 0.15 eV for UPS ($h\nu=21.2$ eV) and 1.2 eV for XPS ($h\nu=1253.6$ eV). The base pressure in the spectrometer was 2×10^{-10} Torr. During operation of the gas discharge lamp for UPS the pressure rose to 1×10^{-9} Torr. The UPS spectra, obtained at 21.2 eV with He I radiation, were recorded with the photons incident at 45° measured from the sample normal and the analyzer was set to register electrons emitted at a normal direction from the sample. The analyzer was operated in the constant-resolution mode with a pass energy of 10 eV for He I radiation. The XPS spectra were obtained with a Mg $K\alpha$ x-ray source. The radiation was incident at 45° and the XPS spectra have been measured at an emission angle of 15°. The analyzer was again operated in the constant-resolution mode with a pass energy of 50 eV.

Before iridium deposition, the cleanliness of the Si substrates was investigated with XPS. The O 1s and C 1s core excitations were not descernible from the background noise, indicating surface contaminations of less than 1% of a monolayer of oxygen or carbon. After surface analysis the composition of the silicide films was analyzed with Rutherford backscattering spectrometry (RBS). The silicide compounds were identified with glancing-angle x-ray diffraction in a Seeman-Bohlin camera. The microstructure of the silicide films was investigated with transmission electron microscopy (TEM) in a Philips 420 STEM (scanning TEM) instrument. The point resolution of the instrument is 3 Å. Samples for TEM analysis were prepared by thinning from the back side with a dimpler to a thickness of about 2 μm. Thinning to the final thickness for TEM analysis was performed in a Gatan 600 ion miller with the sample holder cooled to near-liquid-nitrogen temperature.

III. RESULTS AND DISCUSSION

We have reported in paper I on the electronic structure of the three iridium silicides. The crystal structures of the thermodynamically stable iridium silicides IrSi and $IrSi_3$ are known. IrSi and $IrSi_3$ are the metallic silicide compounds that form at low (400—600 °C) and high ($\simeq$1000 °C) temperatures, respectively. The crystal structure of the semiconducting $IrSi_x$ ($x\simeq1.6$), which forms in the intermediate temperature range, is not yet fully characterized. We have investigated all three silicide compounds with RBS and x-ray diffraction and reported for x a value of 1.6 ± 0.05 (paper I). However, we do not attempt to assign a chemical formula to $IrSi_x$ ($x\simeq1.6$) because of its incomplete structure characterization.

A. Characterization of the interface

Valence-band spectra after sequential deposition of submonolayer quantities of iridium on Si(100) are shown in Fig. 1. They were obtained in normal emission at a photon energy of 21.2 eV. The incident light was unpolarized. Included in Fig. 1 are the valence-band spectra of UHV cleaned Si(100) (bottom spectrum) and of a 650-Å-thick polycrystalline iridium film (top spectrum). These two spectra have been discussed in detail in paper I. Here we will limit their description to a brief summary of various spectral features.

The photoemission spectrum of Si(100)-(2×1) has a dominant peak at 0.7 eV below E_F and a shoulder at −1.3 eV which originate from surface states.[24] The other emission features are associated with bulk transitions. The peaks at −2.4, −3.0, and −3.9 eV are related to p states, the peak at −7.6 eV and the shoulder at −6.8 eV are due to emissions from p states with s admixture, and the weak feature at −9.3 eV is associated with s states.[25] The strong emission in the valence-band spectrum of iridium with two dominant peaks at −0.9 and −4.1 eV and the shoulder at −2.3 eV is due to emission from d states.[26] The shoulder at −1.8 eV is associated with the uppermost valence band[26] and the weak feature at −10.9 eV originates from a minor adsorption of carbon monoxide.[27]

An iridium deposition of only 0.1 Å causes a dramatic modification of the clean Si(100) valence-band spectrum. Most striking are the almost complete disappearance of the intrinsic surface-state peak at −0.7 eV and the loss of the surface-state feature at −1.3 eV. This is strong evidence that a small number of iridium atoms readily

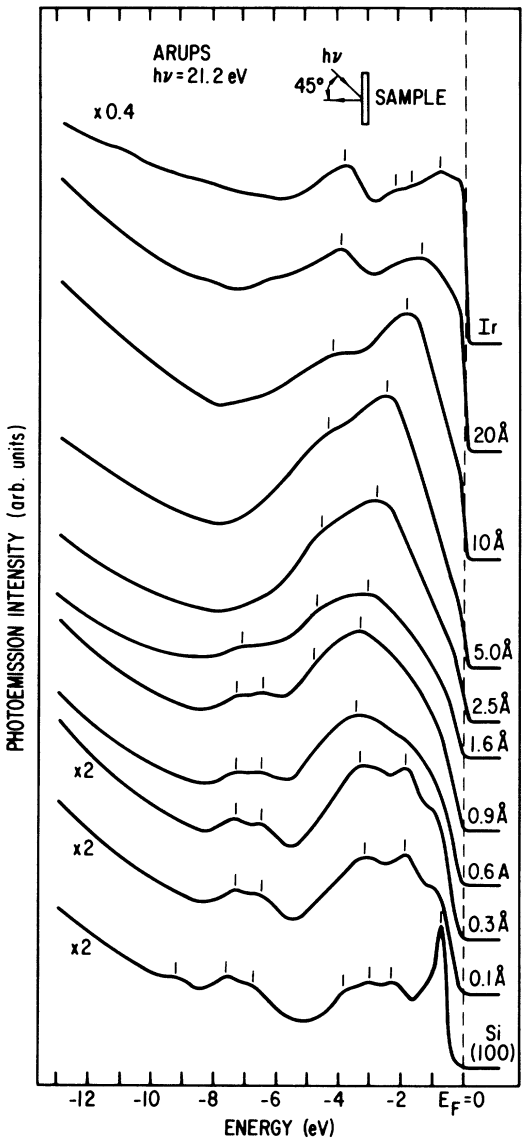

FIG. 1. Valence-band photoelectron spectrum of the clean Si(100) surface and corresponding spectra obtained following sequential deposition of iridium at room temperature. For comparison, the valence-band spectrum of a 650-Å-thick polycrystalline iridium film is included. All spectra were obtained in normal emission at a photon energy of $h\nu=21.2$ eV. The meaning of thicknesses below 1 Å is explained in the text.

change the (2×1) reconstruction of the clean Si(100) surface. Furthermore, the peak at -3.9 eV originating from the valence band and the feature at -9.3 eV associated with *s*-like states have disappeared too. These observations indicate that the interaction between iridium and the topmost silicon atoms is strong and results in the removal of the surface reconstruction. In addition, the remaining emission peaks associated with *p* and *sp* states are shifted to lower binding energy by 0.25—0.38 eV with respect to clean Si(100) which is a result of the band bending as discussed later. The interaction with iridium creates a more metal-like silicon surface as is evident from the strong reduction of the energy gap near E_F.

An increase of the iridium coverage to 0.3 Å produces less dramatic changes in the valence-band spectrum. The intensity of the emission in the region -0.5 to -5.5 eV has increased due to emission from metal *d* states. This trend is clearly visible for larger coverages and is caused by the large photoionization cross section of the *d* states and the larger number of valence electrons of iridium relative to silicon. Particularly, the peak at -3.3 eV has increased and also shifted to higher binding energy. The other emission peaks at -1.8, -6.4, and -7.2 eV have not changed.

At a coverage of 0.6 Å the valence-band spectrum becomes distinctly dominated by the metal *d* states. The peak at -1.8 eV associated with Si *p*—like states has disappeared and intense emission in a broad region of -0.5 to -5.5 eV with a peak at -3.4 eV is visible. However, the emission features at -6.4 and -7.2 eV originating from *s*-*p* states have not changed and remain visible at even higher coverages. An iridium coverage of 0.9 Å further enhances emission from the Ir $5d$ band and produces a new emission feature at -4.7 eV. This feature which starts off as a shoulder at low coverages, develops into a distinct peak and gradually shifts towards lower binding energy with higher coverages. The *d* band emission peak at -3.2 eV has also shifted towards lower binding energy and continues to do so with increased iridium coverages.

An iridium coverage of 1.6 Å produces a valence-band spectrum that has striking resemblance with that of IrSi (see paper I and Fig. 5). The well-defined spectral features at -3.1, -4.6, and -7.0 eV agree well with those observed in bulk IrSi. A difference in the spectra exists near E_F. While IrSi showed a well-defined Fermi edge the spectrum in Fig. 1 displays a very small intensity at E_F. The photoemission spectrum of bulk IrSi was obtained from a 1800-Å-thick layer whereas in the present case the layer thickness is only 1.6 Å. Since the escape depth of 21.2-eV photoelectrons in silicon is about 5 Å (Ref. 25), a considerable contribution of the Si substrate is present in the spectrum of Fig. 1 which explains the relative low density of states at E_F. Thus, we conclude that at a coverage of 1.6 Å the photoemission spectrum clearly points to the formation of an IrSi-like silicide at the interface. As we shall see below, however, the atomic structure at the interface may not be the same as in bulk IrSi.

Further increases in iridium coverage result in the development of spectral features that are specific to metallic iridium. The emission features at -2.8 and -4.5 eV for an iridium coverage of 2.5 Å shift towards lower binding energy with increasing iridium coverage and evolve into the two dominant *d* band peaks of the iridium spectrum shown in the top part of Fig. 1. In addition, a well-defined Fermi edge is discernible at an iridium coverage of 2.5 Å and the density of states at E_F gradually increases with increasing coverage. These observations demonstrate unambiguously the metal enrichment of the surface and the evolution of an unreacted iridium layer at the surface. This trend continues for increasing iridium

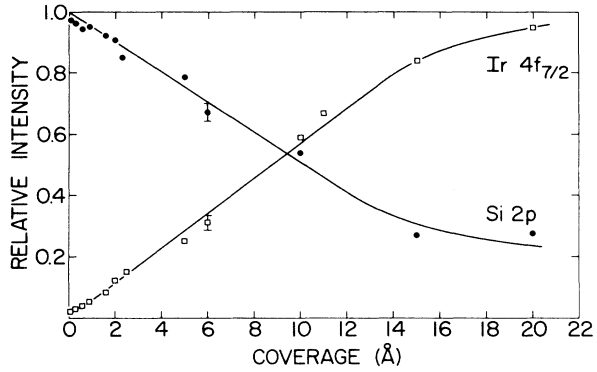

FIG. 2. Relative intensities of the Ir $4f_{7/2}$ and Si $2p$ core-level transitions vs iridium coverage at room temperature.

coverages and is clearly supported by the valence-band spectra obtained for coverages of 5 and 10 Å. At an iridium coverage of 20 Å the valence-band spectrum has a close resemblance to that of a 650-Å-thick polycrystalline iridium film.

Additional information about the reactivity of the Ir/Si interface can be obtained by investigating core-level transitions of iridium and silicon with x-ray photoemission. In Fig. 2 we present the relative intensities of the Ir $4f_{7/2}$ and the Si $2p$ transitions as a function of iridium coverage. In the absence of atomic intermixing of iridium and silicon at the interface the attenuation of the Si $2p$ transition should follow an exponentially decreasing curve and the intensity profile of the Ir $4f_{7/2}$ transition should rise asymptotically to one if it is assumed that the escape depth of the electrons is unaltered by subsequent coverages. Indeed, the exponential decay of the Si $L_{2,3}VV$ Auger intensity with coverage for the unmixed Ag/Si(111) interface[28] shows that a constant escape depth is a valid assumption. Thus, the departure from an exponential behavior in Fig. 2 is a clear sign of the intermixing of iridium and silicon atoms across the Ir/Si interface.

The presence of chemical bonding between iridium and silicon atoms is deducible from the chemical shifts of the corresponding core lines. Figure 3 illustrates the dependence of the chemical shift ΔE_B and of the asymmetry parameter a/b of the Ir $4f_{7/2}$ core line on iridium coverage. ΔE_B is calculated relative to the binding energy of pure iridium and the definition of the asymmetry parameter has been given in paper I. The latter is the quotient of the variances of two different Gaussian distributions fitted to the line shape and as such is a measure of the asymmetrical shape of the core line. A value of one represents a perfectly symmetric line shape. The progressive decrease of chemical shift of the Ir $4f_{7/2}$ core line with increasing iridium coverage reflects the transition from submonolayer coverages of iridium on silicon to bulk iridium. Since band bending effects are negligible for coverages above 2 Å, the continuous shift towards lower binding energies is due to compositional changes from a region of mixed iridium and silicon atoms to a region of bulk iridium. The binding energy approaches that of pure iridium for coverages over 15 Å. At these coverages the iridium atoms see very few silicon neighbors so that the chemical environment of the iridium atoms is no longer influenced by the presence of dilute silicon atoms. The chemical shift of the Ir $4f_{7/2}$ level at a coverage of 1.6 Å is different from the one observed in bulk IrSi (paper I). At such low coverages the difference in chemical shift is due to a combination of band bending and possible deviations of the local atomic arrangements at the interface from that in bulk IrSi. The presence of an IrSi-like silicide at the interface is also supported by the trend in the asymmetry parameter of the Ir $4f_{7/2}$ core line. At low coverages the asymmetry parameter is close to one, pointing to a low density of states at E_F (paper I). The low Fermi-level state densities for low iridium coverages is evident in Fig. 1 and is characteristic of the silicides of iridium (paper I). With increasing metal coverage the surface becomes more metallic and the density of states at E_F increases. This results in a larger asymmetry parameter of the Ir $4f_{7/2}$ core line which is in agreement with the trend observed in Fig. 3.

The energy shift of the Si $2p$ core line is shown in Fig. 4. Again, ΔE_B is calculated relative to the binding energy of pure silicon. Because the escape depth of electrons at a photon energy of 1253.6 eV is 30 Å (Ref. 25), which is much smaller than the depletion layer thickness of the silicon ($\sim 1\ \mu$m), the Si $2p$ core line probes the electronic

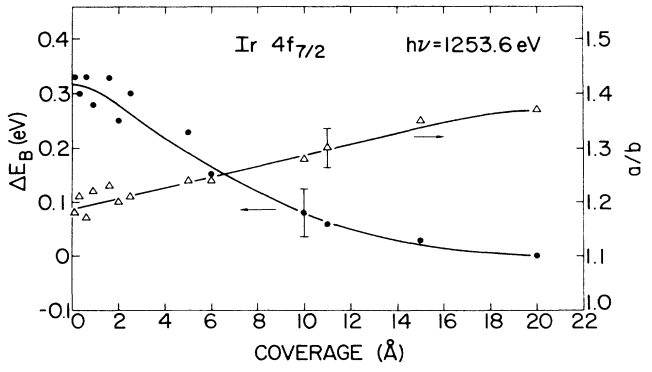

FIG. 3. Dependence of the chemical shift ΔE_B and the asymmetry parameter a/b of the Ir $4f_{7/2}$ core line on iridium coverage. ΔE_B is calculated relative to the binding energy of pure iridium ($E_B^{\mathrm{Ir}} = 60.80 \pm 0.05$ eV).

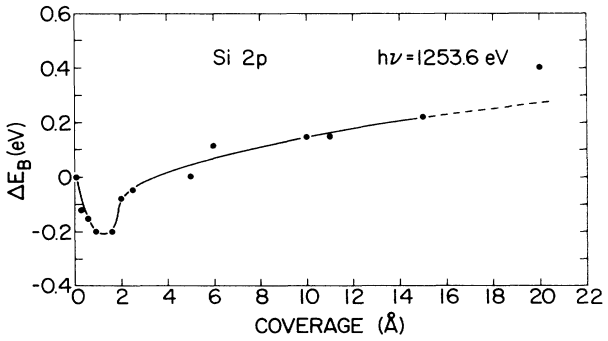

FIG. 4. Dependence of the chemical shift ΔE_B of the Si $2p$ core line on iridium coverage. ΔE_B is calculated relative to the binding energy of pure silicon ($E_B^{\mathrm{Si}} = 99.50 \pm 0.05$ eV).

structure of the Ir/Si interface. Figure 4 shows a clear trend to decreasing binding energy for iridium coverages below 1.0 Å that reverses for coverages around 2.0 Å and changes into a trend to increasing binding energy for high iridium coverages. The valence-band spectrum of Fig. 1 for an iridium coverage of 1.6 Å indicates that a IrSi-like silicide is formed. The negative Si $2p$ core-level shift for iridium coverages below 1 Å does not originate from the bonding between Ir and Si atoms, because the chemical shift is positive for all iridium silicides (see Table I in paper I). Rather, the negative shift is related to an increase in surface band bending and consequently to the evolution of the Schottky barrier at the IrSi/Si interface. Since the energy of the Si $2p$ core level is measured with respect to E_F, the shift of -0.2 eV is representative of a change in the band bending at the interface relative to E_F by the same amount. The implications of this result for the formation of the Schottky barrier will be presented in Sec. III E. At a coverage of about 2.0 Å of iridium the increase in the Si $2p$ binding energy indicates the formation of the IrSi-like silicide. From the valence-band spectra of Fig. 1 we know that at higher converges a metallic iridium overlayer is formed whose thickness increases with increasing iridium coverage. This renders the measurements of the Si $2p$ core level more interface sensitive and is responsible for the slow increase in the Si $2p$ binding energy above 2 Å of iridium coverage. The Si $2p$ core-level shift should approach the value of 0.3 eV measured for bulk IrSi (paper I) as indicated by the dashed line in Fig. 4, but the decrease in the intensity of this core level for thick iridium coverages results in a larger inaccuracy. We have not attempted to determine the asymmetry parameter of the Si $2p$ core line because the limited resolution of our instrument does not permit us to resolve the spin-orbit split Si $2p$ doublet.

B. Sequential formation of the silicide compounds

Thin-film studies have shown[19] that the iridium silicides IrSi, $IrSi_x$ ($x \simeq 1.6$), and $IrSi_3$ form subsequently in different temperature regimes. In the following we will demonstrate that this is consistent with the changes observed in the valence-band spectra of an *in situ* annealed 50-Å-thick film of iridium. More important, we will show the growth and disappearance of the semiconducting compound $IrSi_x$ ($x \simeq 1.6$). For this purpose we have annealed the same sample consecutively at higher temperatures in the range of 400—1100 °C. We have repeated the experiment and found that the results are perfectly reproducible. The annealing time was 5 min. It was kept constant throughout the annealing cycles.

The valence-band spectrum of the unannealed sample and corresponding spectra obtained after subsequent heat treatments are shown in Fig. 5. Additional spectra at intermediate temperatures were obtained but are not included in Fig. 5 because the relative changes in the spectra are not important. The valence-band spectrum of the 50-Å-thick iridium layer deposited on Si(100) is indistinguishable from that of bulk polycrystalline iridium (see Fig. 1). No change in the valence-band spectrum was observed when this sample was annealed at 400 °C. However, annealing at 450 °C causes some noticeable spectral changes. The overall intensity of the d band emission decreases and both the peak at -0.9 eV and the density of states at E_F drop considerably. The spectral features at -2.3 and -4.1 eV shift slightly to higher binding energies and a new feature appears at -8.0 eV. A subsequent heat treatment at 510 °C causes the loss of the d band peak at -0.9 eV and a significant reduction of the other d band peak at -4.3 eV. The visible bottom of the d band that was at about -5.8 eV for the unannealed iridium film is now found at -6.2 eV. These changes are a clear indication of the formation of bonding orbitals between Ir d states and Si sp hybrids as discussed in paper I.

An additional heat treatment at 560 °C produces a valence-band spectrum that is identical to that of IrSi (paper I). The spectral features agree very well with those

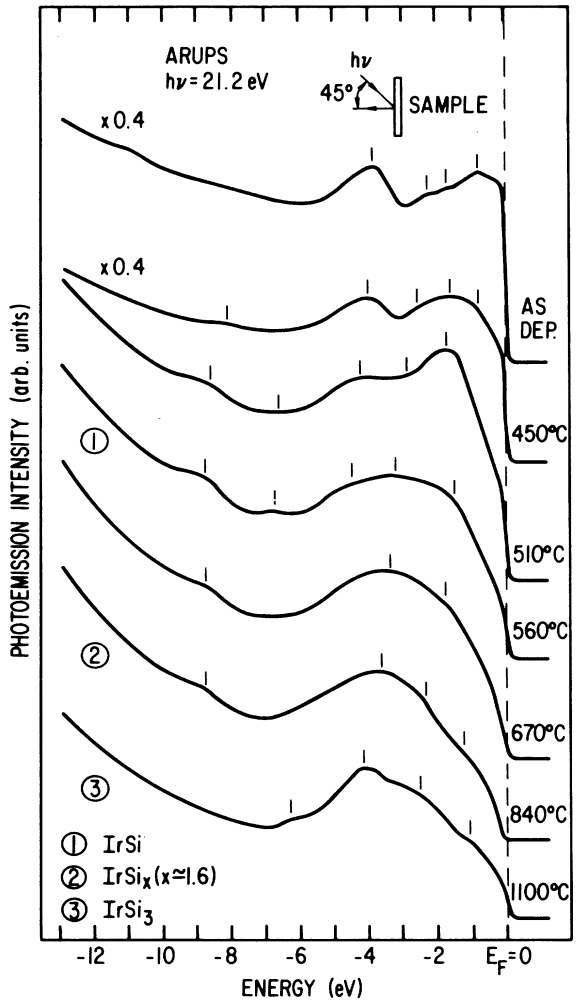

FIG. 5. Valence-band photoelectron spectrum of a Si(100) sample covered with 50 Å of iridium at room temperature and corresponding spectra obtained after annealing the same sample *in situ* at consecutively higher temperatures in the range of 400—1100 °C. The annealing time was 5 min and the spectra were obtained in normal emission at a photon energy of $h\nu = 21.2$ eV.

observed in bulk IrSi and the Fermi edge is clearly visible in Fig. 5. Composition analysis from the core-level intensities of iridium and silicon as well as the chemical shifts of the core-level transitions confirm that the silicide compound formed is IrSi. Further annealing at 670 °C results in a valence-band spectrum that still resembles that of IrSi but shows a much lower density of states at E_F. The development of an energy gap at E_F is clearly seen after an additional heat treatment at 840 °C. This evolution shows the transition from metallic to semiconducting behavior. The overall shape of the spectrum and the spectral features at -1.3, -2.4, -3.6, and -8.9 eV are characteristic of the semiconducting silicide compound $IrSi_x$ ($x \simeq 1.6$) (paper I). The formation of this compound is also confirmed from the analysis of core-level intensities and chemical shifts of iridium and silicon core lines.

The growth of the silicon rich silicide compound $IrSi_3$ is found after a final heat treatment at 1100 °C. The phase $IrSi_3$ is clearly identified by the valence-band spectrum and the core-level data. The existence of a well-defined Fermi edge demonstrates the transition from the semiconducting character of $IrSi_x$ ($x \simeq 1.6$) to the metallic character of $IrSi_3$. At this point, we would like to emphasize that the spectra of Fig. 5 were obtained from a single sample that has been annealed sequentially at higher temperatures. Thus, the valence-band spectra shown in Fig. 5 illustrate clearly the metal-semiconductor-metal transitions accompanying the formation of the three thermodynamically stable iridium silicide compounds. Also, they demonstrate the sequential formation of the iridium silicide compounds in the order of IrSi, $IrSi_x$ ($x \simeq 1.6$), and $IrSi_3$ in the temperature range of 400–1100 °C.

C. Work-function measurements

We have measured the work function ϕ of surface layers by monitoring the secondary electron cutoff in UPS mode and correcting for the work function of the analyzer. The accuracy of this method is about ± 20 meV. Table I lists the work function of Ir, Si(100), and its silicides. The value of $\phi = 4.91$ eV for UHV cleaned Si(100) is in excellent agreement with the result obtained by Allen[29] using the contact potential difference method. Also, $\phi = 5.65$ eV for a thick polycrystalline film of Ir agrees well with the value of 5.67 eV published for Ir(100)[30] but is lower than that of 5.76 eV reported for Ir(111).[31] However, the published values were obtained with field emission measurements. The agreement between different experimental methods is not always satisfactory. Table I shows that there is a dependence of the work function on the composition of the silicide compound. The semiconducting $IrSi_x$ ($x \simeq 1.6$) was found to have the lowest work function. Both $IrSi_x$ ($x \simeq 1.6$) and $IrSi_3$ have a work function that is lower than that of Si(100) whereas the work function of IrSi is close to that of Si(100).

TABLE I. Work function ϕ and Schottky-barrier height ϕ_{Bn} of iridium and its silicides. RT denotes room temperature.

Material	ϕ (eV)	ϕ_{Bn}[a] (eV) Si(100)	Si(111)
Ir(dep. at RT)	5.65±0.02	0.93	0.90
IrSi	4.93±0.02	0.93	0.91
$IrSi_x$ ($x \simeq 1.6$)	4.81±0.02	0.85	0.83
$IrSi_3$	4.88±0.02	0.94	0.92
Si(100)	4.91±0.02		

[a]Reference: I. Ohdomari *et al.*, J. Appl. Phys. **50**, 7020 (1979); J. de Sousa Pires *et al.*, Appl Phys. Lett. **35**, 202 (1979).

The dependence of the surface work function on iridium coverage is shown in Fig. 6. The work function increases linearly at low coverages and saturates at a value close to that for bulk iridium at high coverages. At low coverages, the straight line guiding the eye in Fig. 6 intersects the ordinate at 4.85 eV. This value of the work function is lower than that of 4.91 eV measured for the reconstructed Si(100) surface[29] and may be attributed to the unreconstructed surface. We recall here that an iridium coverage of 0.1 Å readily removes the surface features in the valence-band spectrum of Si(100) pointing to the loss of the surface reconstruction. Indeed, the work function of crystalline silicon is dependent on the surface reconstruction. For Si(111) surfaces for example, a difference in ϕ of about 0.18 eV was observed between the (2×1) and (7×7) reconstructed surfaces.[32] The linear dependence of the work function on iridium coverages below 7 Å is in general agreement with the typical behavior found in the low-coverage regime of an adsorbate on metals.[33] At low coverages where the distance between adatoms is large the dipole moment per adsorbed iridium atom is independent of coverage and consequently the work function change shows a linear dependence on coverage.

At an iridium coverage of 1.6 Å the work function has a value of 4.94 eV as shown in Fig. 6. This value is practically identical to that of IrSi (see Table I) and strongly supports the formation of an IrSi-like phase at a very low iridium coverage. In contrast, a significant delay in the onset of changes of ϕ and the attainment of the value of Pd_2Si has been found for Pd coverages on Si(111).[6] Thus, it appears that the initial stages of the Ir-Si interface formation are different from those of the Pd-Si interface.

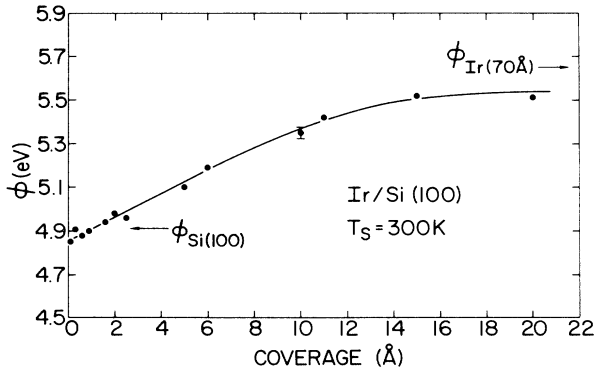

FIG. 6. Dependence of the surface work function ϕ on iridium coverage. The work function was derived from the secondary electron cutoff in UPS mode. Note the absence of a delay in the onset of changes of ϕ with iridium coverage.

D. Microstructural investigation

Transmission electron microscopy analysis of surface layers and thin films provides complementary information to results obtained with photoelectron spectroscopy. The interpretation of valence-band and core-level data depend crucially on the knowledge of the morphology of surface layers and the microstructure and composition of thin films. For this reason we have investigated as-deposited as well as *in situ* annealed films of iridium on Si(100) with TEM.

In Fig. 7 we present a bright-field micrograph and the corresponding electron diffraction pattern of a 5-Å-thick iridium film deposited in situ the UHV chamber onto a clean Si(100) substrate. A very fine surface structure that is homogeneously distributed is readily apparent in the bright-field micrograph. None of the investigated samples with 5- and 6-Å deposits of iridium showed island formation. Thus, we conclude that a 5 Å or thicker film of iridium deposited on Si(100) is homogeneous. Using dark-field imaging we estimate a feature size of about 10 Å of the surface structure of the deposit.

The electron diffraction pattern in Fig. 7 exhibits two diffuse ring patterns as well as matrix spots from the Si(100) substrate. A third diffraction ring is visible on the negative but could not be reproduced in Fig. 7. The matrix spots closest to the transmitted beam are the 220 diffraction spots of the silicon lattice. They can be used to accurately determine the camera length which is necessary for the analysis of the ring pattern. The inner ring corresponds to a d spacing of 3.145 Å and the outer to one of 1.927 Å. The largest d spacing of iridium is found for diffraction of (111) planes and amounts to 2.2170 Å (Ref. 34). Thus, the inner ring cannot originate from iridium. The d spacing associated with this inner ring is close to the d spacing of 3.13 Å for the 002 diffraction of IrSi.[35] Likewise, the d spacing associated with the outer ring agrees well with that of 1.9197 Å for the 200 diffraction of iridium. In conclusion, the electron diffraction pattern of a 5-Å-thick iridium film on Si(100) demonstrates that iridium and silicon atoms at the Ir/Si interface reacted with each other to a limited extend to form a few monolayers of IrSi-like silicide beneath some monolayers of unreacted iridium. This result is in excellent agreement with the interpretation of the valence-band spectra shown in Fig. 1. Whether the structure of the IrSi phase is crystalline or amorphous is yet unclear. Reaction between iridium and silicon during sample preparation for TEM analysis can be ruled out because the samples were cooled to near-liquid-nitrogen temperature during ion milling.

The compounds and their microstructure that form during *in situ* annealing of a 50-Å-thick iridium film on Si(100) are identified in Fig. 8. The electron diffraction pattern and the corresponding bright-field micrograph were taken at the same spot of the sample. The compound formed at 560 °C is clearly identified as IrSi by its diffraction pattern.[35] The numerous spots in the diffraction pattern point to a very fine-grained microstructure which is verified by the bright-field micrograph. The average grain size was found to range between 100 and 300 Å. At 840 °C, the diffraction pattern confirms the formation of the semiconducting silicide $IrSi_x$ ($x \simeq 1.6$) (Refs. 19 and 22). The grain size shown in the corresponding bright-field micrograph is larger than that of IrSi due to the higher temperature of silicide formation. It ranges between 250 and 550 Å. The strong twin-

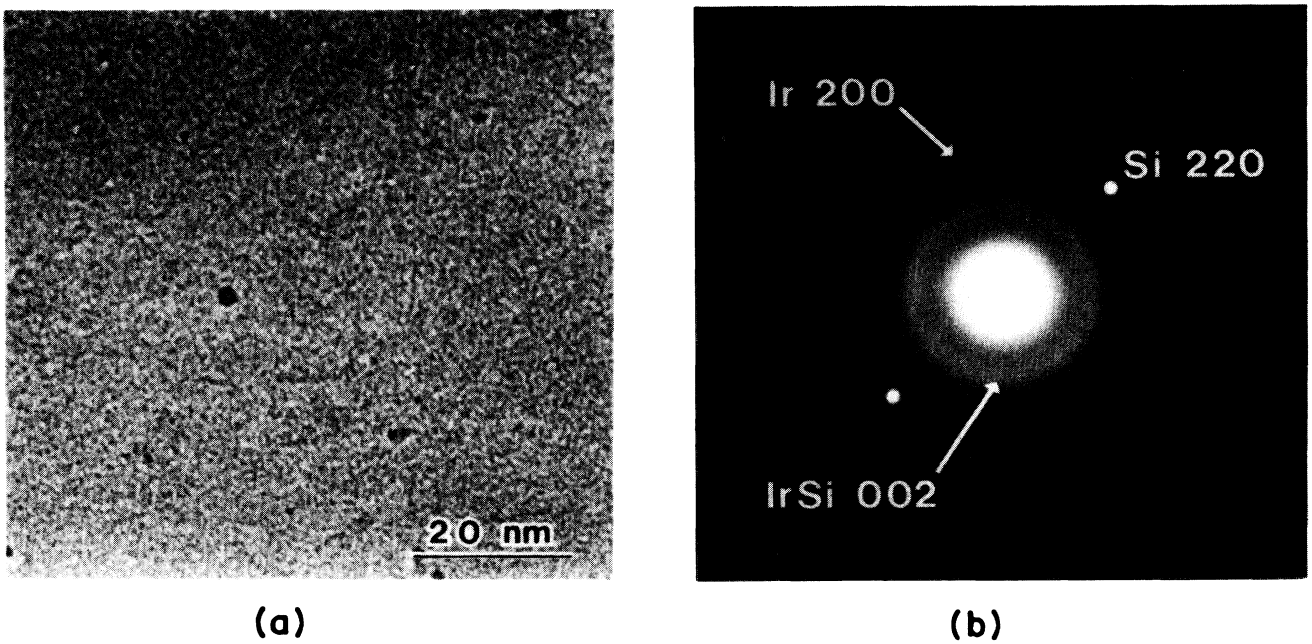

FIG. 7. Bright-field micrograph and corresponding electron diffraction pattern of a 5-Å-thick iridium film as deposited on a Si(100) substrate. The spots in the diffraction pattern are matrix spots of the silicon lattice. The inner diffraction ring originates from IrSi and the outer ring from unreacted iridium.

ning observable in some of the grains might be responsible for the many weak diffraction spots that are discernible in the diffraction pattern. The very large unit cell of this compound causes also a large number of closely spaced diffraction rings. Finally, at 1100 °C the diffraction pattern verifies the formation of $IrSi_3$ (Ref. 36). Its microstructure is polycrystalline with a grain size ranging from 500 to 1300 Å as shown by the bright-field micrograph. Annealing at 1100 °C for periods longer than 5 min can lead to island formation of the $IrSi_3$. We observed this ef-

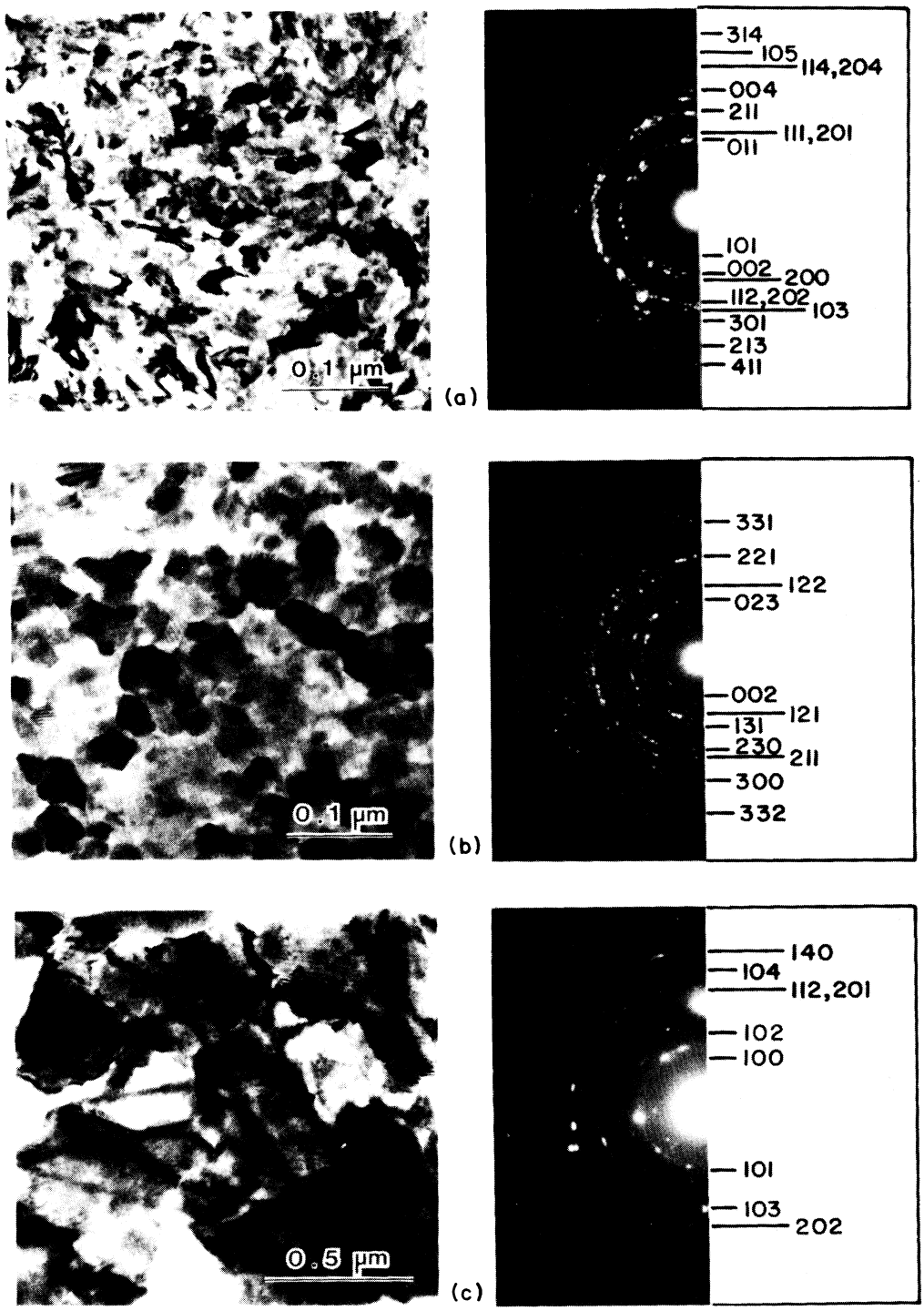

FIG. 8. Bright-field micrograph and corresponding electron diffraction pattern of 50-Å-thick iridium films on Si(100) anealed *in situ* at 560 °C, 840 °C, and 1100 °C, respectively. The compounds formed are clearly identified as (a) IrSi, (b) $IrSi_x$, ($x \simeq 1.6$), and (c) $IrSi_3$ by the indexing of their diffraction pattern.

fect with UPS which showed a valence-band spectrum that resembled a superposition of $IrSi_3$ and Si spectra and confirmed it with TEM analysis.

E. Discussion

The above results provide ample evidence that submonolayers of iridium react with Si(100) substrates at room temperature. First of all, the disappearance of the silicon surface state features and the disappearance and energy shift of bulk silicon emission peaks are clear signs that a coverage of 0.1 Å of iridium not only alters the (2×1) surface reconstruction but also increases the band bending. The change in surface reconstruction implies that bonding occurred between iridium and silicon atoms. The change in the relative intensities of the core-level transitions with increasing iridium coverage indeed points to a mixing of iridium and silicon atoms across the Ir/Si interface. The formation of bonding orbitals can be inferred from the chemical shifts of the core-level lines. However, the chemical shift of the Ir $4f_{7/2}$ level for submonolayer coverages relative to bulk iridium is not necessarily a sign of chemical interaction because of differences in the atomic structures, but in combination with the shift of the Si $2p$ level, which points to the formation of a silicide phase, a chemical reaction of iridium with silicon can be deduced. In addition, the valence-band spectrum for an iridium coverage of 1.6 Å cannot be explained as a simple superposition of pure silicon and pure iridium valence-band spectra. Rather, it resembles that of bulk IrSi as mentioned before. These facts not only support chemical reaction but also rule out island formation of iridium on silicon. Final proof of chemical reaction between iridium and silicon is provided by the electron diffraction pattern in Fig. 7 which reveals the presence of IrSi at the Ir/Si interface. A reactive Ir/Si interface is consistent with most metal-silicon interfaces that have been investigated to date. Even the V/Si (Ref. 10) and Ti/Si (Ref. 11) interfaces that were first reported to be nonreactive have recently been found to form compounds.[37] The Ag/Si(111) interface is probably the only known nonreactive metal-silicon interface.[28] Finally, we would like to point out that the bright-field micrograph in Fig. 7 shows that a deposit of 5 Å of iridium on Si(100) is homogeneous. The valence-band spectra suggest that this is also the case for deposits below 5 Å thickness.

The room-temperature reaction of iridium and silicon is limited. The reaction starts at the interface and progressively diminishes further away from the interface due to the build up of a pure iridium overlayer. This is evident from both the valence-band spectra of Fig. 1 and the electron diffraction pattern of Fig. 7. The little change observed in the valence-band spectra for iridium coverages between 0.6 and 1.6 Å is due to the stability of the p-d bonded IrSi silicide (paper I). For iridium coverages above 2 Å the reaction stops and an unreacted iridium overlayer grows as evidenced by the similarity of the valence-band spectra to that of pure iridium. This observation is also a clear proof of the absence of any silicon surface segregation as it seems to occur to a certain extend in the Pd/Si (Ref. 6) and Pt/Si (Ref. 9) systems. The growth kinetics of thin films of IrSi from Ir/Si bilayer couples obeys a parabolic law,[19] which means that the diffusion of the constituent atoms to the reaction interface is the rate limiting mechanism. In our case, it is therefore possible that the limited extend of the Ir-Si reaction is due to the low diffusivity of iridium and silicon atoms at room temperature. Finally, it is noteworthy to mention that the gradual buildup of the Fermi edge with increased coverage and the lack of changes in the density of states near E_F point to the absence of interface states below E_F.

Extended reaction between iridium and silicon can be obtained by annealing a thin iridium layer deposited on a silicon substrate. The valence-band spectra presented in Fig. 5 and the TEM results shown in Fig. 8 demonstrate that only one silicide compound forms at a time. This sequential formation of silicide compounds during slow heating is a characteristic of most thin-film transition-metal–silicon systems.[38] This is in contrast to rapid thermal annealing which is known to produce multiple compounds as well as metastable silicides.[39] In the present case we confirm the formation of three silicides in the sequence of IrSi, $IrSi_x$ ($x\simeq1.6$), and $IrSi_3$ as reported earlier.[19,20] However, we have demonstrated the transitions from a metallic to a semiconducting and a semiconducting to a metallic silicide with increasing temperature of annealing. This unique feature of the Ir-Si system has not been observed in other transition-metal silicides.

So far our discussion has provided a detailed picture of the chemical reactions occurring at the Ir/Si interface. We will now address the implications of this picture on the formation of the Schottky barrier. For this purpose we have listed the published barrier heights of iridium deposited at room temperature and its silicides on Si(100) and Si(111) substrates[20,40] in Table I. First of all, it is interesting to note that the barrier heights of Ir and IrSi are the same within the experimental accuracy of ±0.01 eV. This is not surprising and agrees well with our finding of an IrSi-like interfacial layer. We therefore conclude that at room temperature the barrier height of Ir on Si is very much like the barrier height of IrSi on Si. Next, the barrier height of the semiconducting silicide is close to those of the metallic silicides. It is possible that the p-type semiconductor $IrSi_x$ ($x\simeq1.6$) (paper I) becomes metallic by stoichiometric deviations and/or impurities which push the Fermi level into the valence band. The listed barrier heights of $IrSi_x$ ($x\simeq1.6$) are then those of a degenerate semiconductor on Si(100) and Si(111). Last of all, the difference of 20 meV in the barrier heights on Si(100) and Si(111) substrates was not explained in the literature.[20]

For an ideal metal-semiconductor interface that is free of defects and interface states the Schottky model[41] predicts that the barrier height ϕ_{Bn} is the difference between the metal work function ϕ_M and the electron affinity χ_s of the semiconductor, $\phi_{Bn}=\phi_M-\chi_s$. Because of the compound formation, ϕ_M is in this case that of the silicides. With $\chi_s=4.20$ eV (Ref. 42) and the measured values of ϕ_M from Table I we obtain barrier heights of 0.73 eV for IrSi, 0.61 eV for $IrSi_x$ ($x\simeq1.6$), and 0.68 for $IrSi_3$. It is immediately apparent that this simple picture of the Schottky barrier does not agree with the experimen-

tally determined barrier heights. Though we have neglected contributions from surface dipoles, such effects should make a small correction[43] to the calculated value of the barrier height. In contrast, our core-level data agree very well with the measured barrier heights. The Fermi level at the Si(100)-(2×1) surface is 0.41 eV above the valence-band maximum.[44] The band bending of 0.2 eV deduced from the Si 2p core-level shift implies a barrier height of $E_g-(E_F-E_v)+\Delta E_{\mathrm{Si}\,2p}=0.91$ eV. This value agrees very well with the experimentally measured barrier height of IrSi.

Deviations from the Schottky model can be caused by intrinsic or extrinsic surface or interface states. Bardeen[45] suggested that surface states of the clean semiconductor surface might persist under a metal overlayer and pin the Fermi level. In the present case, however, we have clear evidence that the surface states of silicon vanish upon metal coverage and that a subsequent formation of a chemical compound causes a geometric rearrangement of atoms at the metal-silicon interface. It is important to stress at this point that the Schottky barrier is fully developed after deposition of the first monolayer of the metal onto the clean semiconductor surface. This is not only true for the Ir/Si interface but is a generally observed phenomenon.[46] Consequently, we can rule out the presence of intrinsic surface states and have to consider only extrinsic surface states. Extrinsic surface states are new states induced by the metal and can originate from interfacial defects[47–49] and metal-induced gap states.[50] Within the capabilities of our instrumental techniques we have not been able to detect any defect states at the Ir/Si interface. Though their existence is thereby not demonstrated, they might not be ruled out altogether. The kind of interfacial defects that have been proposed for covalent semiconductor-metal interfaces are dangling bonds.[49] However, a direct experimental observation is not possible. Recently, metal-induced gap states received a lot of attention as possible candidates to explain the Schottky-barrier heights of transition metals on group IV semiconductors. For a coverage of one monolayer of metal on silicon it is appropriate to talk of surface states rather than metal-induced gap states. The surface states can pin the Fermi level just as the metal-induced gap states do. With increased metal coverage there is likely to be a continuous transition from surface to metal-induced gap states. However, the Fermi level pinning position may also change and be different for surface states and metal-induced gap states. The nature of the pinning states is thus not clearly identified.

It is not clear which of the models of extrinsic surface states satisfactorily explains the deviation of the iridium-silicide–silicon barrier heights from the classic Schottky model. A common feature of all theoretical models proposed until now is the assumption of a highly idealized metal-silicon interface that is sharp and does not include chemical reactions and diffusive transport of atoms across the interface. These chemical effects, however, are very important in view of the fact that most metal-silicon interfaces are reactive and their influence in the determination of the Schottky-barrier height is not clear. Photoemission spectroscopy investigations of metal-silicon interfaces indicate that these interfaces are much more complicated than generally assumed in theoretical models. Strong diffusive intermixing may result in a graded interface as proposed by Freeouf.[51] In this context it is interesting to note that most theoretical investigations used the experimental results of gold-semiconductor interfaces as test vehicle and in general found satisfactory agreement. However, it is well known that the gold-semiconductor interface is a reactive one,[52] as is expected from the low eutectic temperatures of gold-semiconductor alloys (Au/Si, 363 °C, Ref. 53; Au/Ge, 361 °C, Ref. 54; Au/GaAs, 339 °C, Ref. 55), and that gold is also a fast diffuser in most semiconductors.[56] Because both facts seem inconsistent with a sharp metal-semiconductor interface, the agreement between theoretical Schottky-barrier models and the experimental data of gold-semiconductor contacts is rather astonishing. It remains to be seen whether new experiments and theoretical models are able to finally resolve the nature of the Schottky barrier.

IV. CONCLUSIONS

Our photoelectron spectroscopy and TEM investigation of the Ir/Si interface has shown that submonolayers of iridium react with silicon at room temperature. However, the reaction is limited and for thicker layers leads to the formation of an interfacial silicide resembling IrSi and an unreacted iridium overlayer. We have also demonstrated the subsequent formation of the three thermodynamically stable silicide compounds IrSi, IrSi_x ($x\simeq 1.6$), and IrSi_3 in the temperature range of 400–1100 °C and the concurrent transitions from metallic to semiconducting and semiconducting to metallic behavior. We showed that the simple Schottky model does not correlate our measured work functions with the published barrier heights of the three silicides on n-type silicon. However, our core-level data agrees well with the measured barrier height of IrSi and we were able to explain the identity of the published barrier heights of Ir and IrSi on silicon. Finally, we compared existing theoretical models of the Schottky barrier with our experimental data and suggest that the disruption of the silicon surface by the chemical reactivity of most metal-silicon interfaces may contribute to the pinning of the Fermi level and thus influence the barrier height.

ACKNOWLEDGMENTS

We are grateful to J. L. Freeouf, J. D. Tersoff, and J. F. Morar for fruitful discussions and to S. T. Pantelides for a careful review of the manuscript. One of us (P.O.) would like to thank the IBM Thomas J. Watson Research Laboratory (Yorktown Heights, NY) for making his stay there possible during the course of the work.

*Permanent address: Institute of Physics, University of Basel, Klingelbergstrasse 82 CH-4056 Basel, Switzerland.

[1]J. L. Freeouf, G. W. Rubloff, P. S. Ho, and T. S. Kuan, Phys. Rev. Lett. **43**, 1836 (1979).

[2]J. N. Miller, S. A. Schwarz, I. Lindau, W. E. Spicer, B. DeMichelis, I. Abbati, and L. Braicovich, J. Vac. Sci. Technol. **17**, 920 (1980).

[3]P. J. Grunthaner, F. J. Grunthaner, A. Madhukar, and J. W. Mayer, J. Vac. Sci. Technol. **19**, 649 (1981).

[4]G. V. Hansson, R. Z. Bachrach, R. S. Bauer, and P. Chiaradia, Phys. Rev. Lett. **46**, 1033 (1981).

[5]P. S. Ho, P. E. Schmid, and H. Föll, Phys. Rev. Lett. **46**, 782 (1981).

[6]G. W. Rubloff, P. S. Ho, J. L. Freeouf, and J. E. Lewis, Phys. Rev. B **23**, 4183 (1981).

[7]I. Abbati, G. Rossi, I. Lindau, and W. E. Spicer, J. Vac. Sci. Technol. **19**, 636 (1981).

[8]A. Franciosi, D. J. Peterman, and J. H. Weaver, J. Vac. Sci. Technol. **19**, 657 (1981).

[9]G. Rossi, I. Abbati, L. Braicovich, I. Lindau, and W. E. Spicer, Phys. Rev. B **25**, 3627 (1982).

[10]J. G. Clabes, G. W. Rubloff, and T. Y. Tan, Phys. Rev. B **29**, 1540 (1984).

[11]R. Butz, G. W. Rubloff, T. Y. Tan, and P. S. Ho, Phys. Rev. B **30**, 5421 (1984).

[12]H. F. Liu, H. M. Liu, and T. T. Tsong, Phys. Rev. Lett. **56**, 65 (1986).

[13]R. A. Butera, M. del Gindice, and J. H. Weaver, Phys. Rev. B **33**, 5435 (1986).

[14]J. Ihm, M. L. Cohen, and J. R. Chelikowsky, Phys. Rev. B **22**, 4610 (1980).

[15]O. Bisi and K. N. Tu, Phys. Rev. Lett. **52**, 1633 (1984).

[16]O. Bisi, L. W. Chiao, and K. N. Tu, Phys. Rev. B **30**, 4664 (1984).

[17]J. Robertson, J. Phys. C **18**, 947 (1985).

[18]D. R. Hamann and L. F. Mattheiss, Phys. Rev. Lett. **54**, 2517 (1985).

[19]S. Peterson, J. Baglin, W. Hammer, F. d'Heurle, T. S. Kuan, I. Ohdomari, J. de Sousa Pires, and P. Tove, J. Appl. Phys. **50**, 3357 (1979).

[20]I. Ohdomari, K. N. Tu, F. M. d'Heurle, T. S. Kuan, and S. Peterson, Appl. Phys. Lett. **33**, 1028 (1978); I. Ohdomari, T. S. Kuan, and K. N. Tu, J. Appl. Phys. **50**, 7020 (1979).

[21]M. Wittmer, P. Oelhafen, and K. N. Tu, Phys. Rev. B **33**, 5391 (1986).

[22]S. Peterson, J. A. Reimer, M. H. Brodsky, D. R. Campbell, F. d'Heurle, B. Karlsson, and P. A. Tove, J. Appl. Phys. **53**, 3342 (1982).

[23]W.-K. Chu, J. W. Mayer, and M.-A. Nicolet, *Backscattering Spectrometry* (Academic, New York, 1978), p. 89.

[24]F. J. Himpsel and D. E. Eastman, J. Vac. Sci. Technol. **16**, 1297 (1979); R. I. G. Uhrberg, G. V. Hansson, J. M. Nicholls, and S. A. Flodström, Phys. Rev. B **24**, 4684 (1981); J. E. Rowe and H. Ibach, Phys. Rev. Lett. **32**, 421 (1974).

[25]L. Ley, M. Cardona, and R. A. Pollak, in *Photoemission in Solids II*, Vol. 27 of *Topics in Applied Physics*, edited by L. Ley and M. Cardona (Springer, New York, 1979), p. 11.

[26]J. F. van der Veen, F. J. Himpsel, and D. E. Eastman, Phys. Rev. B **22**, 4226 (1980).

[27]T. N. Rhodin, J. Kanski, and C. Brucker, Solid State Commun. **23**, 723 (1977).

[28]G. LeLay, Surf. Sci. **132**, 169 (1983); M. Hanbücken and G. LeLay, *ibid.* **168**, 122 (1986).

[29]F. G. Allen, J. Phys. Chem. Solids **8**, 119 (1959).

[30]B. E. Nieuwenhuys. R. Bouwman, and W. M. H. Sachtler, Thin Solid Films **21**, 51 (1974).

[31]R. W. Strayer, W. Mackie, and L. W. Swanson, Surf. Sci. **34**, 225 (1973).

[32]M. Erbudak and T. E. Fischer, Phys. Rev. Lett. **29**, 732 (1972); F. J. Himpsel, P. Heimann, T.-C. Chiang, and D. E. Eastman, *ibid.* **45**, 1112 (1980).

[33]J. C. Fuggle and D. Menzel, Surf. Sci. **53**, 21 (1975); H. A. Engelhardt and D. Menzel, *ibid.* **57**, 591 (1976).

[34]Powder Diffraction File No. 6-0598, Joint Committee on Powder Diffraction Standards (International Center for Diffraction Data, Swarthmore, 1984).

[35]Powder Diffraction File No. 10-206, Joint Committee on Powder Diffraction Standards (International Center for Diffraction Data, Swarthmore, 1984).

[36]Powder Diffraction File No. 19-598, Joint Committee on Powder Diffraction Standards (International Center for Diffraction Data, Swarthmore, 1984).

[37]E. J. van Loenen, A. E. M. J. Fisher, and J. F. van der Veen, Surf. Sci. **155**, 65 (1985); J. Vähäkangas, Y. U. Idzerda, E. D. Williams, and R. L. Park, Phys. Rev. B **33**, 8716 (1986); R. A. Butera, M. del Giudice, and J. H. Weaver, *ibid.* **33**, 5435 (1986); J. H. Weaver (private communications).

[38]F. M. d'Heurle and P. Gas, J. Mater. Res. **1**, 205 (1986).

[39]M. Wittmer and G. A. Rozgonyi, *Current Topics in Materials Science*, edited by E. Kaldis (North-Holland, Amsterdam, 1982), Vol. 8, p. 1, and references therein.

[40]J. de Sousa Pires, P. Ali, B. Crowder, F. d'Heurle, S. Peterson, L. Stolt, and P. A. Tove, Appl. Phys. Lett. **35**, 202 (1979).

[41]W. Schottky, Naturwiss. **26**, 843 (1938); Z. Phys. **113**, 367 (1939).

[42]The electron affinity can be calculated from $\chi_s = \phi + (E_F - E_V) - E_g$. With our measured value of $\phi = 4.91$ eV, $E_F - E_V = 0.41$ eV from Ref. 44 and $E_g = 1.12$ eV at 300 K we obtain $\chi_s = 4.20$ eV, in excellent agreement with values for Si(111) published by C. A. Sebenne, Nuovo Cimento **39**, 768 (1977). To our knowledge values for Si(100) are not known.

[43]C. A. Mead, Solid-State Electron. **9**, 1023 (1966); M. Schlüter, J. Vac. Sci. Technol. **15**, 1374 (1978).

[44]J. F. Morar (private communication): The Si $2p$ core level for the Si(100)-(2×1) surface is shifted by −0.22 eV from that of the Si(111)-(7×7) surface. The Fermi-level position at the Si(111)-(7×7) surface is 0.63 eV above E_v (Ref. 32).

[45]J. Bardeen, Phys. Rev. **71**, 717 (1947).

[46]W. Mönch, Surf. Sci. **21**, 443 (1970); J. L. Freeouf, M. Aono, F. J. Himpsel, and D. E. Eastman, J. Vac. Sci. Technol. **19**, 681 (1981).

[47]A. Zur, T. C. McGill, and D. L. Smith, Phys. Rev. B **28**, 2060 (1983); A. Zur and T. C. McGill, J. Vac. Sci. Technol. B **2**, 440 (1984).

[48]W. E. Spicer, I. Lindau, P. R. Skeath, C. Y. Su, and P. W. Chye, Phys. Rev. Lett. **44**, 420 (1980); W. E. Spicer, P. W. Chye, P. R. Skeath, C. Y. Su, and I. Lindau, J. Vac. Sci. Technol. **16**, 1422 (1979).

[49]O. F. Sankey, R. E. Allen, and J. D. Dow, Solid State Commun. **49**, 1 (1984); O. F. Sankey, R. E. Allen, and J. D. Dow, J. Vac. Sci. Technol. B **2**, 491 (1984), O. F. Sankey, R. E. Allen, S.-F. Ren, and J. D. Dow, *ibid.* B **3**, 1162 (1985).

[50]V. Heine, Phys. Rev. **138** A1689 (1965); S. G. Louie and M. L. Cohen, Phys. Rev. B **13**, 2461 (1976); S. G. Louie, J. R. Chelikowsky, and M. L. Cohen, *ibid.* **15**, 2154 (1977); J. Tersoff, Phys. Rev. Lett. **52**, 465 (1984).

[51]J. L. Freeouf, Solid State Commun. **33**, 1059 (1980); J. Vac.

Sci. Technol. **18**, 910 (1981); Surf. Sci. **132**, 233 (1983).

[52]L. Braicovich, C. M. Garner, P. R. Skeath, C. Y. Su, P. W. Chye, I. Lindau, and W. E. Spicer, Phys. Rev. B **20**, 5131 (1979); P. W. Chye, I. Lindau, P. Pianetta, C. M. Garner, and W. E. Spicer, *ibid.* **17**, 2682 (1978); I. Lindau, P. W. Chye, C. M. Garner, P. Pianette, C. Y. Su, and W. E. Spicer, J. Vac. Sci. Technol. **15**, 1332 (1978); L. J. Brillson, Phys. Rev. B **18**, 2431 (1978).

[53]H. Okamoto and T. B. Massalski, Bull. Alloy Phase Diagrams **4**, 190 (1983).

[54]H. Okamoto and T. B. Massalski, Bull. Alloy Phase Diagrams **5**, 601 (1984).

[55]R. P. Elliott and F. A. Shunk, Bull. Alloy Phase Diagrams **2**, 356 (1981).

[56]In Si, K. Nakashima, M. Iwami, and A. Hiraki, Thin Solid Films **25**, 423 (1975); M. Hill, M. Leitz, and R. Sittig, J. Eletrochem. Soc. **129**, 1579 (1982); U. Gösele, W. Frank, and A. Seeger, Appl. Phys. **23**, 361 (1980); in Ge, E. N. Mgbenu, Phys. Status Solidi A **53**, 397 (1979); in GaAs, D. Boyer, Y. Limousin, A. Baldy, and J. C. Maire, J. Microsc. Spectrosc. Electron. **3**, 143 (1978); L. J. Brillson, R. S. Bauer, R. Z. Bachrach, and G. Hansson, Phys. Rev. B **23**, 6204 (1981).

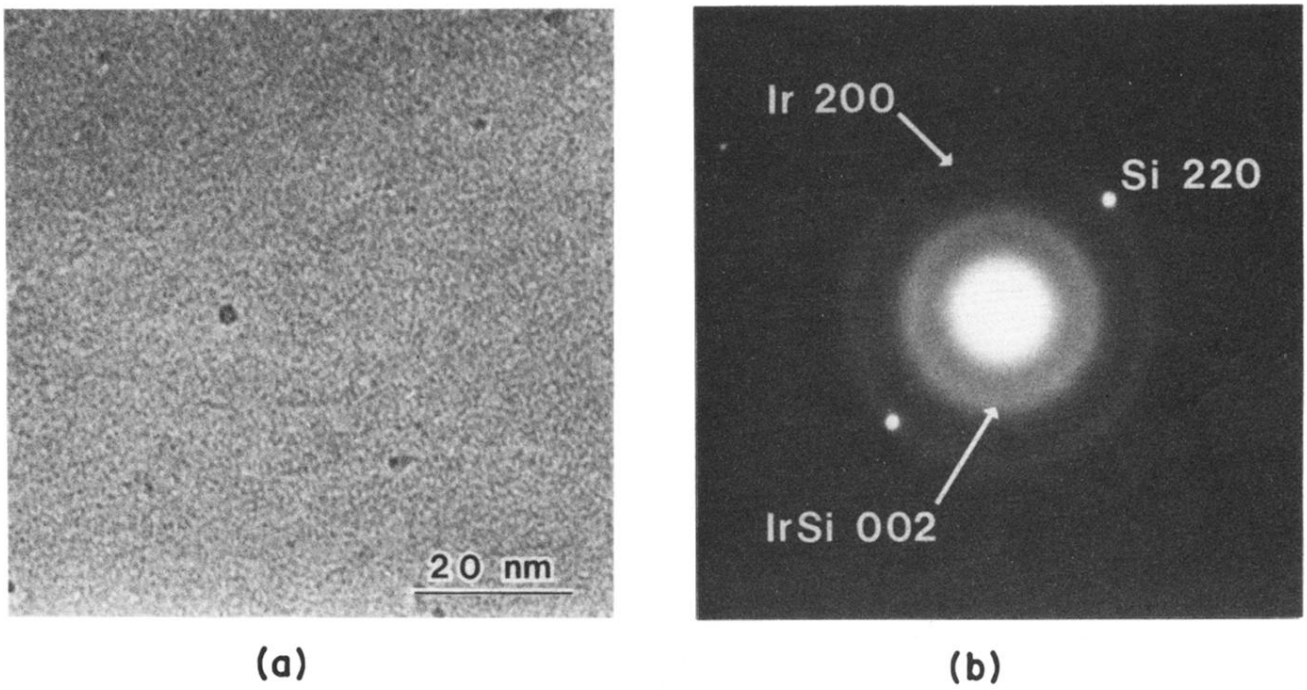

FIG. 7. Bright-field micrograph and corresponding electron diffraction pattern of a 5-Å-thick iridium film as deposited on a Si(100) substrate. The spots in the diffraction pattern are matrix spots of the silicon lattice. The inner diffraction ring originates from IrSi and the outer ring from unreacted iridium.

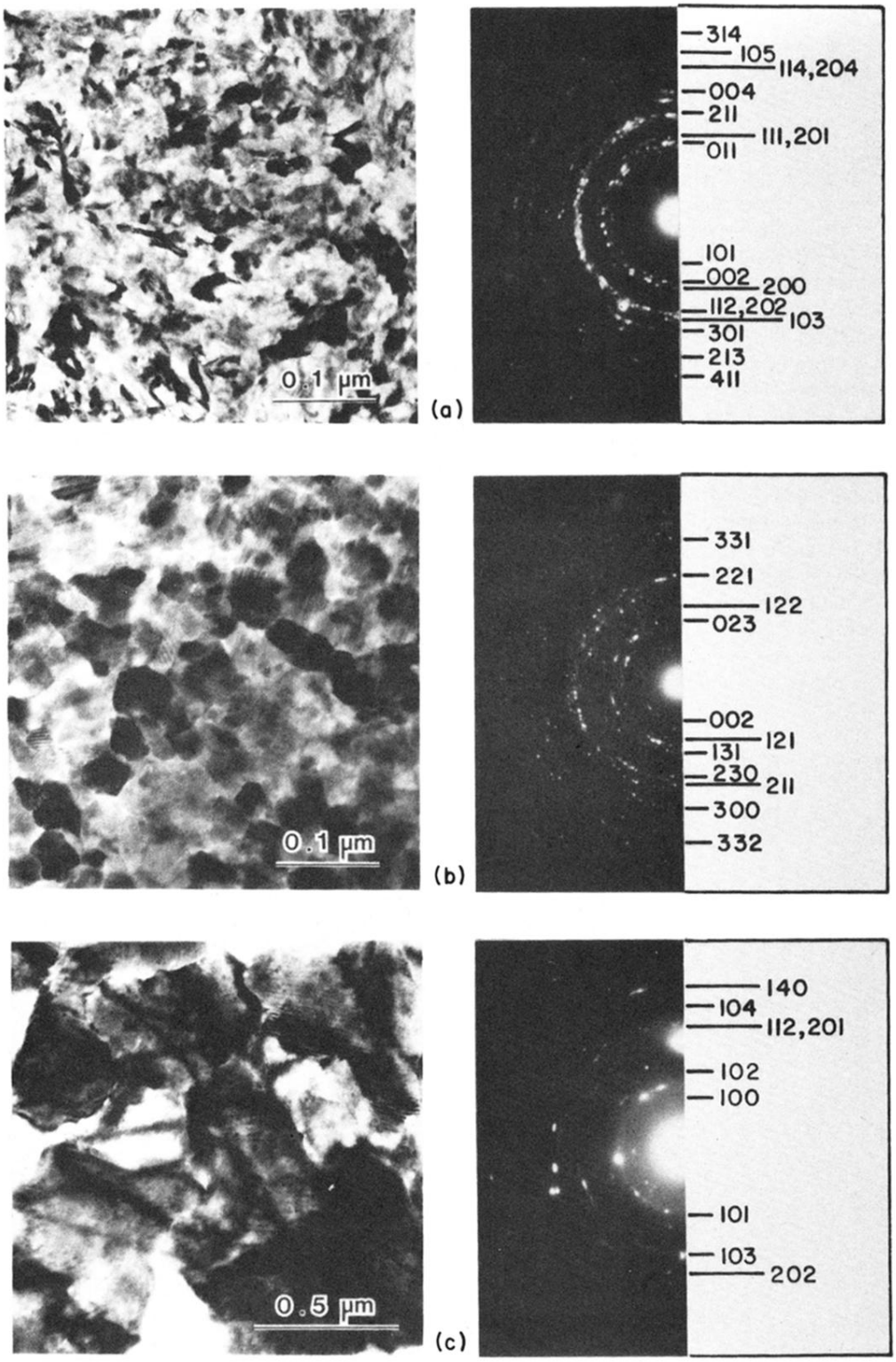

FIG. 8. Bright-field micrograph and corresponding electron diffraction pattern of 50-Å-thick iridium films on Si(100) anealed *in situ* at 560 °C, 840 °C, and 1100 °C, respectively. The compounds formed are clearly identified as (a) IrSi, (b) $IrSi_x$, ($x \simeq 1.6$), and (c) $IrSi_3$ by the indexing of their diffraction pattern.